

Alternately Moving Road Method for the FEM/DEM Simulation of Tire-Sand Interactions

C.L. Zhao, *M.Y. Zang

School of Mechanical & Automotive Engineering, SCUT, Guangzhou 510640, China

*Corresponding author: myzang@scut.edu.cn

Abstract

The Finite-Discrete Element Method (FEM/DEM) is a promising tool to analyze the tire-sand interactions. However, it usually requires a long driving distance to investigate the tire running behavior on the sand road which will lead to a large-scale simulation model. The Alternately Moving Road Method is proposed in this study to reduce the size of the simulation model: the sand road which has been passed over by the tire is removed and same size of road specimen is laid in front of the tire simultaneously. This method possesses the ability to keep the road scale constant and acceptable in the simulation of arbitrary length sand roads. Numerical model of tire driving on sand road is established to verify the feasibility of the method. And the simulation results are compared with the current experimental results to validate the feasibility and effectiveness of the method.

Keywords: Alternately Moving Road Method, Tire-sand interactions, FEM/DEM, Running behavior

1 Introduction

The in-depth study of the tire-sand interactions is significant to the design and parameter match of off-road vehicles. Recently, as the rapidly developed of computer technology, numerical method becomes an efficient and economic approach for the research of this field. The Finite Element Method (FEM) and the Discrete Element Method (DEM) are two frequently used methods. The FEM, which is based on the continuous theory, possesses the advantage of describing the tire characteristics [BIRIS et al., (2011); Cuong et al., (2013); González Cueto et al., (2013); Li and Schindler, (2013); Moslem and Hossein, (2014)], and the DEM is appropriate to model the granular futures such as large displacement of the sand [Khot et al., (2007); Knuth et al., (2012); Nakashima et al., (2007); Smith and Peng, (2013); Zhang et al., (2012)]. Thus, it is quite nature to use the DEM and the FEM together (FEM/DEM) to taken into account the advantages of the two method in the investigation of tire-sand interactions, where the sand can be modeled by using the DEM and the tire model can be discretized into finite elements.

The FEM/DEM method has been used by David [David et al., (2001)], Nakashima [Nakashima and Oida, (2004); Nakashima et al., (2008), (2009)] and Zhao [Zhao and Zang, (2014a), (2014b)] to investigate the tire-soil interactions and proved to be an effective tool. In these literatures, the discrete elements were contact with each other and with the finite elements, and the contact detection was the most time consuming part. Although various kinds of contact detection algorithms were applied by researchers to improve the computing efficiency, it is still the bottleneck problem for the application of this method due to large amount of discrete elements, especially for a longish test road. In this study, the 3D FEM/DEM is applied to investigate the tire-sand interactions and the Alternately Moving Road Method (AMRM) is proposed to keep a constant number of discrete elements for the simulation of arbitrary length test

roads.

The structure of the paper is as follows: Sect. 2 briefly introduces the basis for the application of the FEM/DEM to the investigation of the tire running behavior on sand terrain. Sect. 3 illustrates the principle of the AMRM according to two-dimensional schematics. Sect. 4 presents the detailed FEM/DEM numerical example of a rigid tire running on sand road, where the feasibility of the AMRM is also displayed. The conclusions of this study are listed in Sect. 5.

2 The basis for analyzing tire running behavior by using FEM/DEM

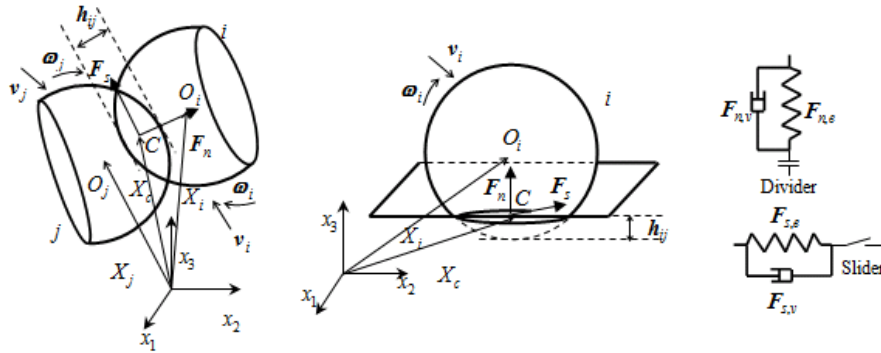
The motions of the discrete elements and the finite element nodes are governed by the Newton's Second Law. For arbitrary element i , the equations are expressed by Eq. (1) (used for both discrete elements and finite element nodes) and Eq. (2) (only used for discrete elements).

$$m_i(d^2\mathbf{u}_i / dt^2) = \mathbf{F}_i \quad (1)$$

$$I_i(d^2\boldsymbol{\theta}_i / dt^2) = \mathbf{M}_i \quad (2)$$

where m_i and I_i are the mass and inertia moment of element i , respectively; \mathbf{u}_i and $\boldsymbol{\theta}_i$ are the displacement and the rotation angle of element i , respectively; \mathbf{F}_i and \mathbf{M}_i are the total external force and centroidal moment of element i , respectively. Eqs. (1) and (2) are solved by the explicit finite difference method.

The contact models for elements are shown in Fig. 1, where h_{ij} is the overlap of two contact elements; \mathbf{v}_i , \mathbf{v}_j , $\boldsymbol{\omega}_i$ and $\boldsymbol{\omega}_j$ are the velocity and angular velocity of element i and j , respectively; O_i , O_j are the mass center of the discrete element i and j , respectively; C is the contact point of the elements; \mathbf{F}_n is the normal force, and \mathbf{F}_s , taken Coulomb friction law into account, is the tangential force among elements. $\mathbf{F}_{n,e}$ and $\mathbf{F}_{n,v}$ are the normal spring and the normal damping forces, respectively; $\mathbf{F}_{s,e}$ and $\mathbf{F}_{s,v}$ are the tangential spring and the tangential damping forces, respectively. The spring and damping forces are calculated by the Hertz-Mindlin theory [Balevičius et al., (2004)] for both the two types of contact, where the finite elements are regarded as spheres with infinite radius [Han et al., (2000)]; μ is the friction coefficient.



(a) Discrete elements model (b) Discrete and finite element model (c) Interaction forces
Figure 1. Contact models among elements

The concept of analyzing tire-sand interactions by using the FEM/DEM is illustrated in Fig. 2. The discrete elements contact with each other and with the finite element tire. Consequently, the tire drawbar pull N , vertical reaction force \mathbf{P} and slip ratio s can be derived from Eqs. (3) - (5).

$$N = G - |\mathbf{R}| \quad (3)$$

$$\mathbf{P} = \sum \mathbf{f}_y \quad (4)$$

$$s = (1 - \nu / (r\omega)) \quad (5)$$

where f is the contact force between the finite elements and the discrete elements; $\mathbf{G} = \sum \mathbf{f}_{x+}$ and $\mathbf{R} = \sum \mathbf{f}_{x-}$ are the gross traction force and the resistance, respectively; ν and ω are the translational speed and the angular velocity of the tire; r is the tire radius.

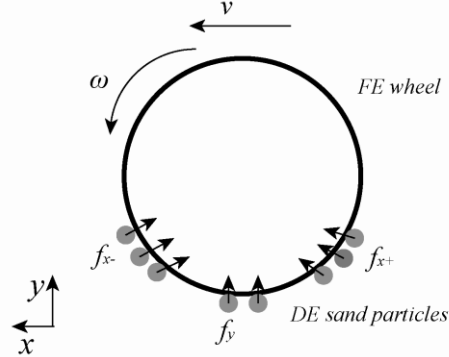


Figure 2. The tire-sand analysis system by using the FEM/DEM

3 The Alternately Moving Road Method

It is obvious that the sand outside a certain distance of the tire center have less influence on the tire running behavior. Thus, during the tire running process, the sand which is run over by the tire could be removed and new sand could be laid in front of tire to form new road. Accordingly, the Alternately Moving Road Method is proposed and the specific steps are as follows: first, the sand road sample, which is a section of the whole road, is established. Then, the initial sand road is assembled by combining two road samples in sequence. After that, the tire is placed on the sand road and starts to run. The alternation is performed when the tire travels a proper distance. The execution flowchart of the method is shown in Fig. 3, where T is the current calculation time; T_{ter} is the termination time, Δt denotes the time step of the explicit time integration.

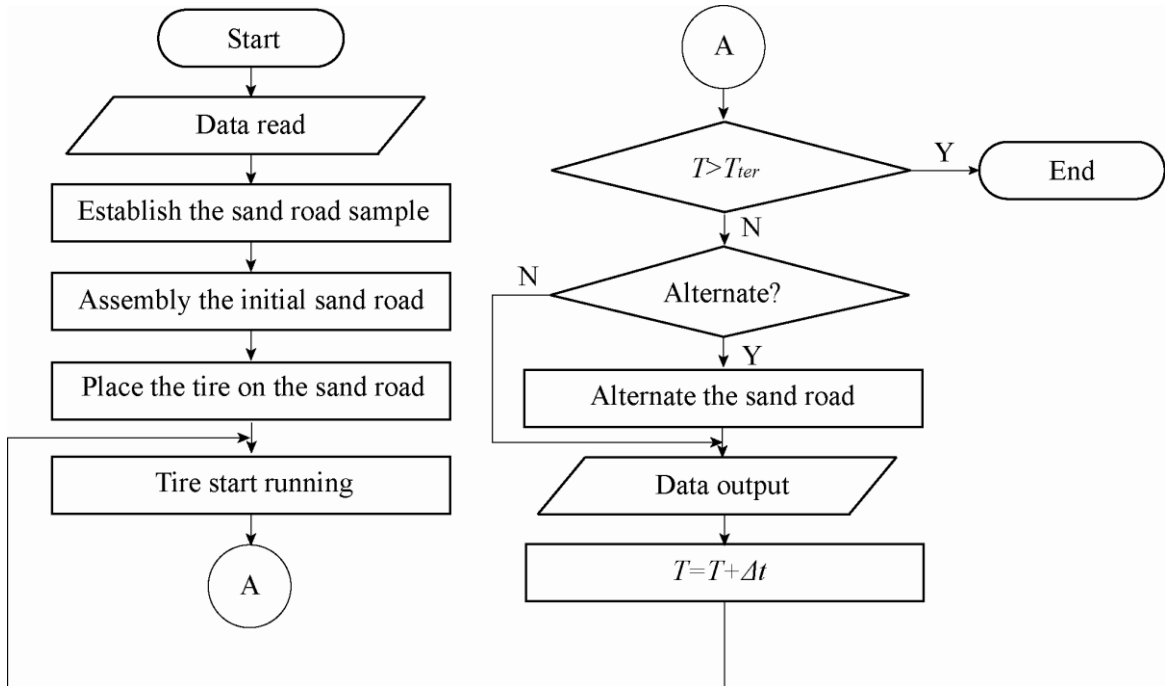


Figure 3. The execution flowchart

3.1 The establishment of sand road sample

Firstly, the discrete elements which are randomly distributed in a given domain are generated. There might be contact among the elements but no overlaps, contact forces or confining stress at this stage. Thus the elements should be rearranged to a steady state under self-weight to simulate the real sand. The boundary of the domain is constrained by rigid walls during the rearrangement process and the C-grid algorithm [Williams et al., (2004)] is applied for the contact detection among the discrete elements. The Discrete Element Set (DES) at the stable stage is the so-called sand road sample (recorded as DES S), as illustrated by two-dimensional schematic in Fig. 4. To facilitate the descriptions later, the element sequence numbers in the schematic are recorded as $1 \sim N$; the coordinates of arbitrary element i are recorded as $X: S_{x,i}$, $Y: S_{y,i}$; the length of the sample is equal to a ; The constraint boundaries of the rigid wall are $X: [0, a]$, $Y: [0, b]$. The contact detection regions for the C-grid algorithm are also set to be $X: [0, a]$, $Y: [0, b]$.



Figure 4. The sand road sample

3.2 The assembly of the initial sand road

The initial sand road consists of two sand road samples mentioned in Sect. 3.1. The sand road sample DES S is duplicated into two DESs and recorded as DES A_0 and DES A_1 . The DES A_0 and DES A_1 are arranged in sequence along the X direction to assemble the initial sand road, as illustrated in Fig. 5. The total element number of the initial sand road is $2N$. This is realized by adding the constant value a to the X coordinate of each element in DES A_1 . Simultaneously, the element sequence numbers of DES A_1 are changed into $N+1 \sim 2N$. The coordinates of arbitrary element i in DES A_1 are $X: S_{x,i-N}+a$, $Y: S_{y,i-N}$. Other parameters of the elements are unchanged. The constraint boundaries of the rigid wall are altered into $X: [0, 2a]$, $Y: [0, b]$. The contact detection regions for the discrete elements are also altered as $X: [0, 2a]$, $Y: [0, b]$.

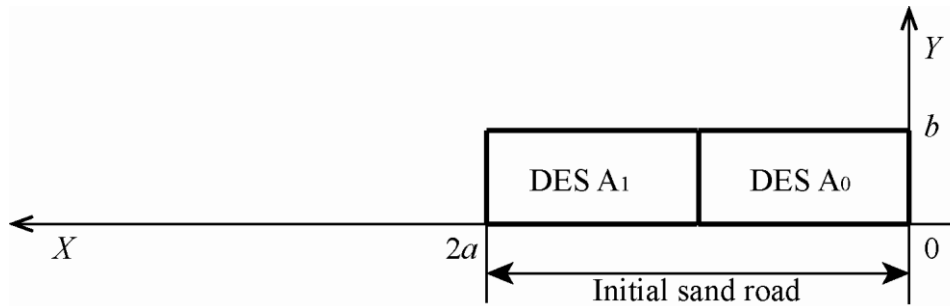


Figure 5. The initial sand road

3.3 The Alternately Moving Road process

The tire is placed at the center position of the DES A_0 , as illustrated in Fig. 6, and

vertical load including self-weight of the tire and external load is loaded to the tire mass center. A constant angular velocity ω and corresponding translational speed v are enforced to the mass center of the tire after the vertical reaction force between the tire and the road is equal to the given vertical load. Then the tire starts to run along the X direction under specific slip ratio conditions.

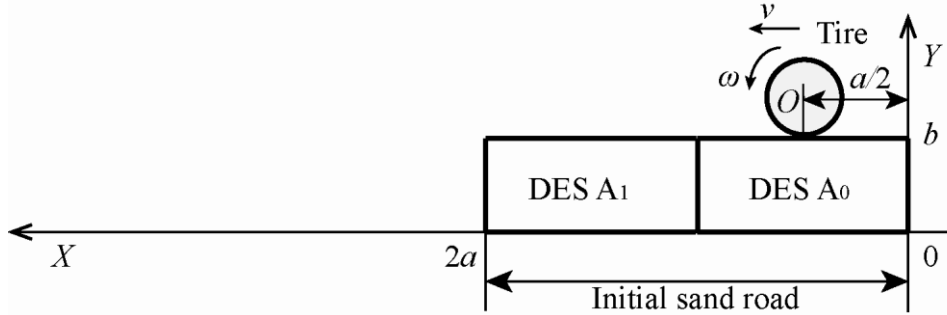


Figure 6. Initial position of the tire

The Alternately Moving Road process is performed when the tire arrives at the alternate point, where DES A_0 has almost no influence on the tire running behavior and the distal end of the DES A_1 is not seriously damaged. In this study, the alternate point is at the center position of the DES A_1 as illustrated in Fig. 7.

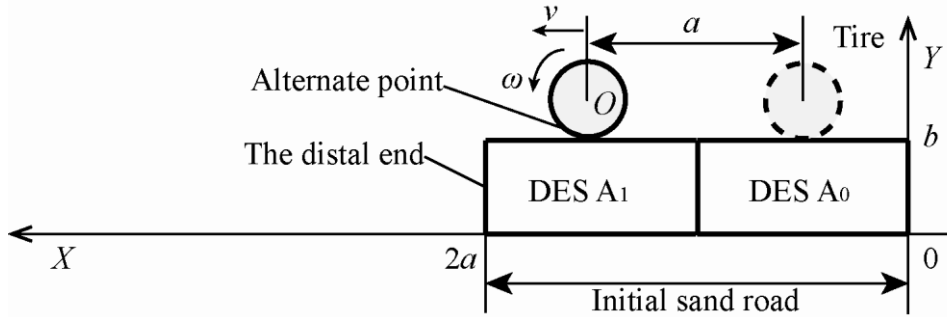


Figure 7. The alternate point for the AMRM

Then the elements of DES A_0 are removed and the road sample DES S (established in Sect. 3.1) is duplicated again and recorded as DES A_2 . The element coordinates of DES A_2 are altered by adding the constant value $2a$ to the X coordinate of each element and the element sequence numbers are recorded as 1 to N . The coordinates of arbitrary element i are $X: S_{xi}+2a, Y: S_{yi}$ after the alternation. Then, the DES A_1 and DES A_2 form a new sand road, as illustrated in Fig. 8. The constraint boundaries of the rigid wall are altered into $X: [0,3a], Y: [0,b]$. The contact detection regions for the discrete elements are also changed into $X: [0,3a], Y: [0,b]$.

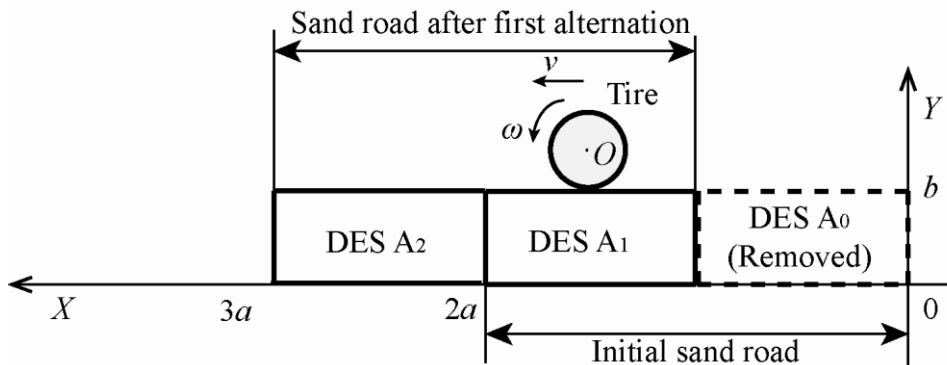


Figure 8. The first time of sand road alternation

Repeat the alternate process along the tire running direction and the tire running behavior on arbitrary length of sand road can be investigated with constant number of discrete elements. The alternate principles are as follows: for the k th alternation, if k is odd, the element sequence number is set to be $1 \sim N$; else if k is even, the element sequence number is set to be $N+1 \sim 2N$; The coordinates for arbitrary element i should be changed into $X: S_{xi}+(k+2)a$, $Y: S_{yi}$ for k is odd, and to be $X: S_{xi-N}+(k+2)a$, $Y: S_{yi-N}$ for k is even; The constraint boundaries of the rigid wall and the contact detection regions for the discrete elements should be changed into $X: [ka, (k+2)a]$, $Y: [0, b]$.

4 Numerical examples

Three-dimensional numerical model of tire running on sand road is established based on the soil-bin experiment in [Shinone et al., (2010)] to validate the feasibility and effectiveness of the AMRM in the investigation of the tire-sand interactions, where the sand road is modeled by discrete elements and the tire is discretized into finite elements. And the tire running behavior under different slip ratio is also investigated.

4.1 The sand road sample

Firstly, the discrete elements, which are randomly distributed in a given domain of $X: [0, 735]$, $Y: [0, 480]$, $Z: [0, 280]$, are generated, as illustrated in Fig. 9. The friction coefficient between the discrete element and the rigid wall is set to be 0.3. The displacement contour of the discrete elements in Z direction during the rearrangement process under self-weight is shown in Fig. 10. The time history of the total gravitational potential energy (TGPE) is shown in Fig. 11. The value shows a decreasing trend and tends to be stable after 1.1 s of rearrangement. Then the rearrangement process is completed. The porosity value for the final state is about 0.32. The discrete element set is stored as the road sample. It should be noticed that this paper is focusing on the validation of the effectiveness of the AMRM, thus the radius range of the discrete element is 6~7 mm which is larger than the real sand.

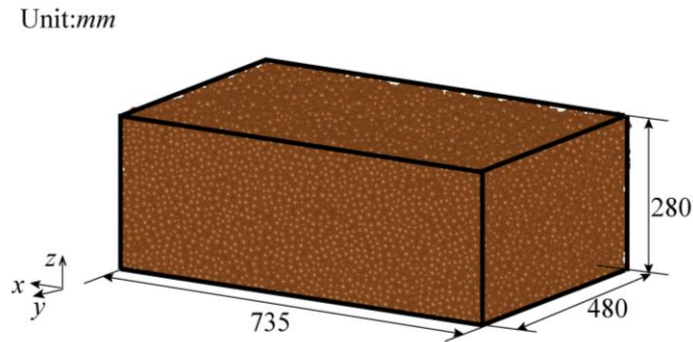
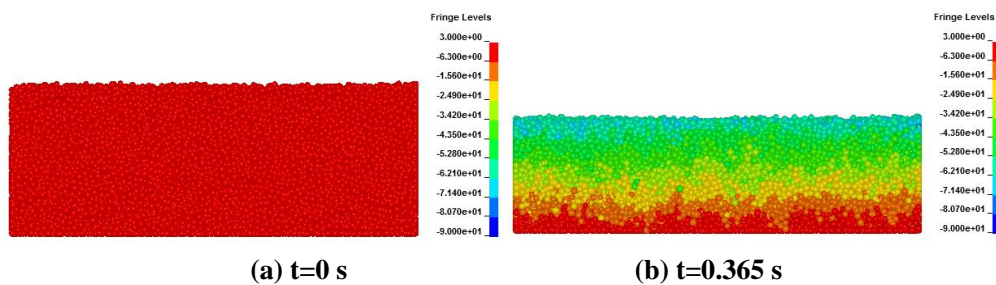


Figure 9. The configuration of the discrete element after the initial generation

Discrete element parameter: Young's Modulus: 75000 MPa, Poisson's Ratio: 0.3, Density: 2400 kg/m³, Element number: 45551, Friction coefficient: 0.3.



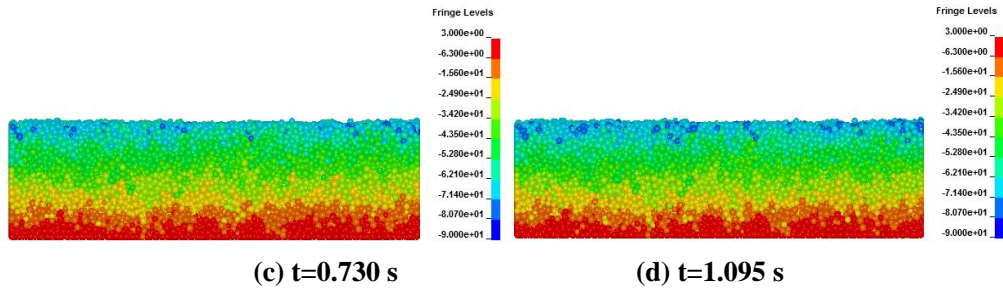


Figure 10. The displacement counter of the discrete elements in Z direction during the rearrangement process under self-weight (front view)

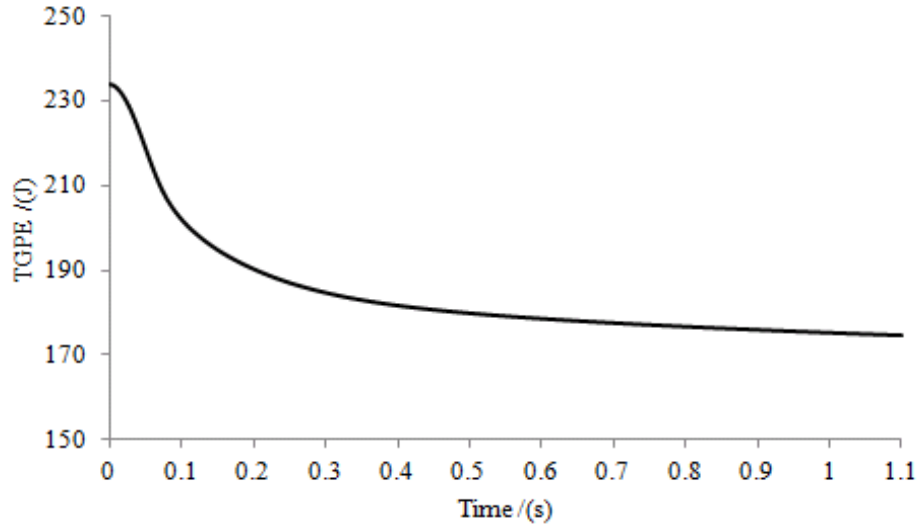


Figure 11. Time history of the TGPE of the discrete elements

4.2 Models of the initial sand road and the tire

The initial sand road consists of two road samples as illustrated in Fig. 12. The model size parameters refer to the soil-bin experiment in [Shinone et al., (2010)]. The discrete element number is 91102, the length of the initial sand road is 1470 mm which is two times of the sand road sample illustrated in Sect. 4.1. The parameters of the discrete elements are the same as the ones in Sect. 4.1.

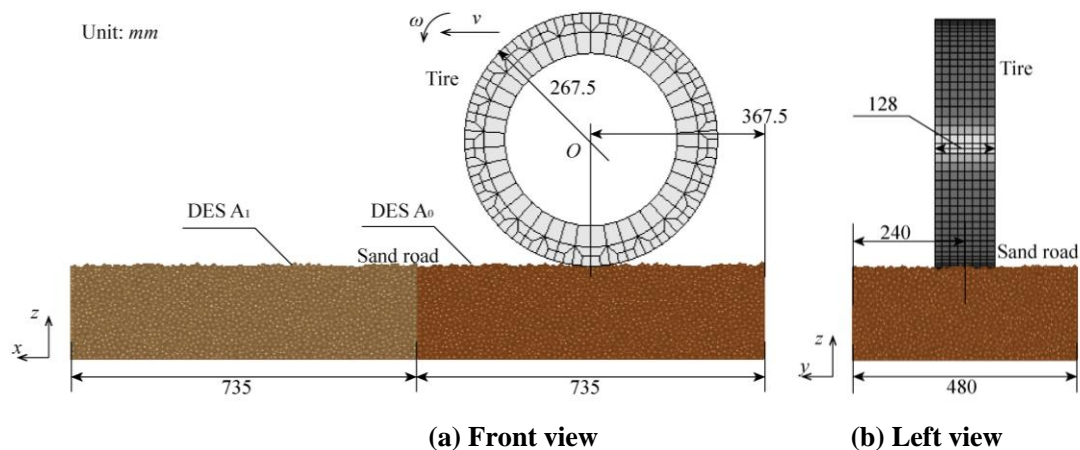


Figure 12. The models of the initial sand road and the finite element tire
 Parameters of the tire: Young's Modulus: 2 MPa, Poisson's Ratio: 0.49, Density: 1800 kg/m³, Element number: 1344.

The tire is placed on the sand road. Vertical load of 1295 N including the self-weight of the tire and the external vertical load is loaded to the center of the tire. The tire

sinks onto the sand road until the vertical reaction force between the tire and road reached 1295 *N*. Afterwards, constant angular velocity of 0.5 *rad/s* and corresponding translational speed are enforced to the tire center, and the tire travels towards the *X* direction under 30% slip ratio. The tire deformation is neglected for the given experimental inflation pressure of the tire in [Shinone et al., (2010)]. The friction coefficient between the tire and the sand road is set to be 0.4.

4.3 The alternately moving road process

The tire running along the *X* direction and the alternation of the sand road is performed when the tire running a distance of $k*735$ mm, where *k* is alternate times. The displacement counter of the discrete elements in *Z* direction during the traveling process is shown in Fig. 13: Fig. 13(a) is the initial configuration; Fig. 13(b) shows the rut of the tire at time 0.777 s; when the tire travels a distance of 735 mm, the first alternation is performed, as shown in Fig. 13(c); then, the tire continues to move, and the rut of the tire at 1.58 s is shown in Fig. 13(d); After 1470 mm of travel, the second alternation is performed, as illustrated in Fig. 13(e); The total tire traveling distance is 1560 mm, and the final configuration is shown Fig. 13(f). During the running process, the length of the sand road keeps a constant value of 1470 mm, the total number of the discrete elements keeps a constant value of 91102.

The simulation is carried out on a PC. The principal characteristics of the PC are Intel Core i3-2100 1.58GHz (CPU), 2.00GB (RAM) and Windows XP Home Basic SP3 32bit. The elapsed time for the above numerical test is approximately 72 hours.

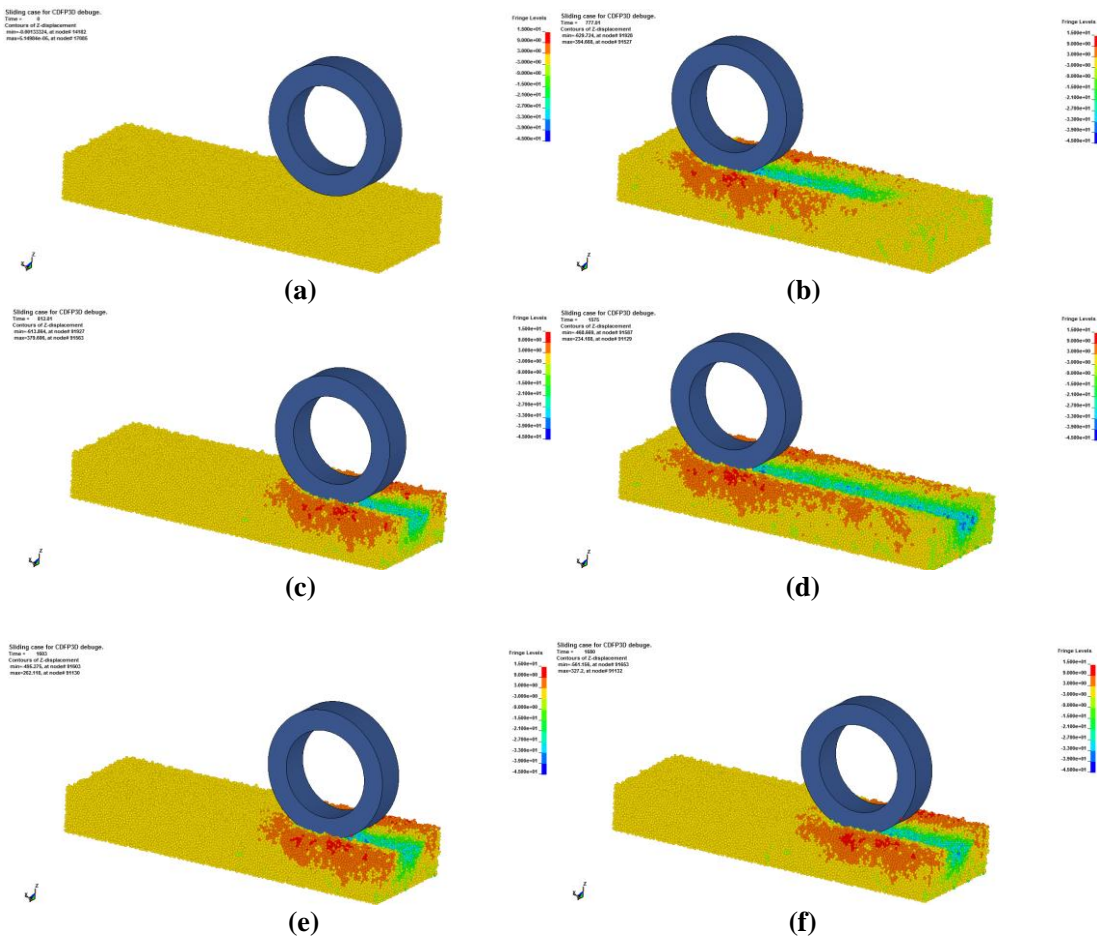


Figure 13. Displacement counter of the discrete elements under the rolling tire in 30% slip ratio

4.4 Tire running behavior

Fig. 14 shows the vertical reaction force as a function of the traveling distance under the 30% slip ratio condition. It can be seen that the vertical reaction force shows an abrupt fluctuation at the initial stage. The possible reason is that there is a vertical downward velocity when the tire was placed on the sand road (see Sect. 4.2 for detail), this lead to an impact between the tire and the road. Afterward, the tire vertical reaction force tend to be stable and its value fluctuates around 1295 N which is the given load value.

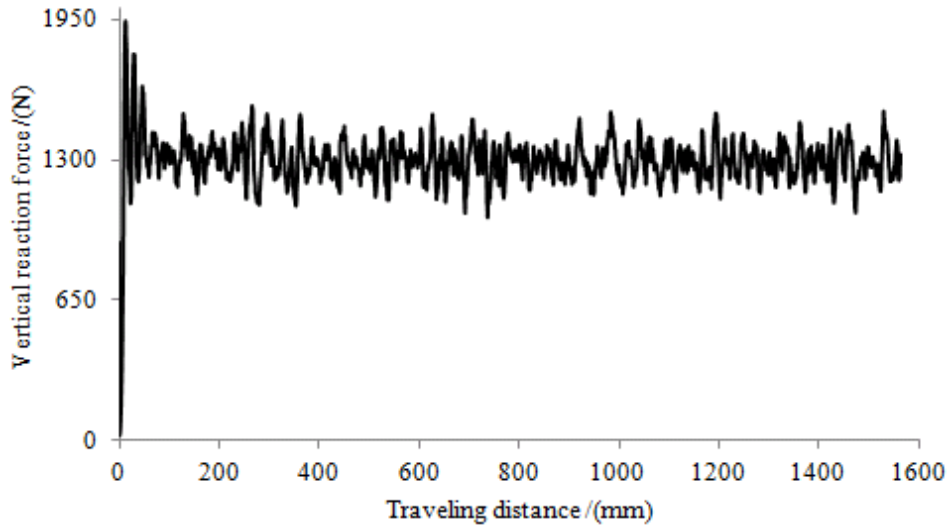


Figure 14. The vertical reaction force during the traveling process

Fig. 15 shows the drawbar pull as a function of the traveling distance under the 30% slip ratio condition. Analogous to the abrupt fluctuations of the vertical reaction force, the drawbar pull also shows a dramatic fluctuation at the initial stage because the tire traction force G is proportional to the vertical reaction force. After that the drawbar pull value is relatively stable without any abrupt fluctuations at the alternate point and its value fluctuates around 75 N. The possible reason for the fluctuations of the drawbar pull is the large radius values of the discrete elements.

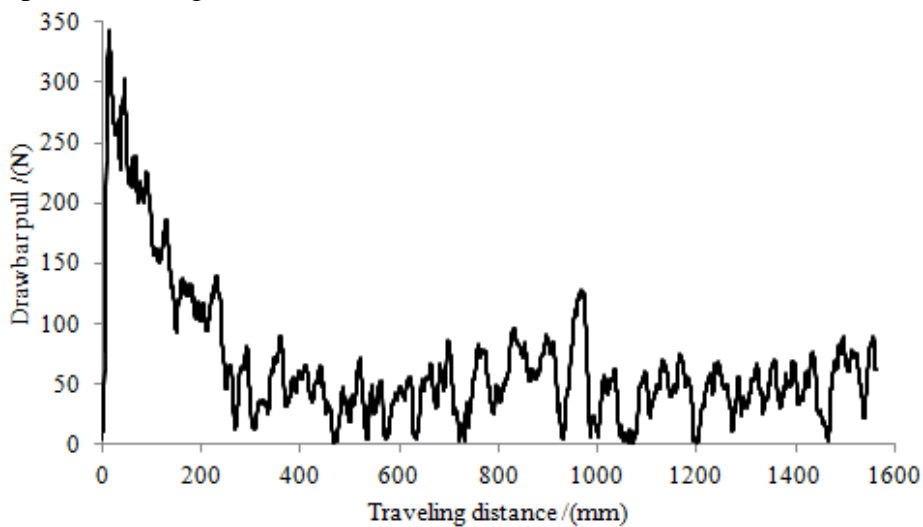


Figure 15. The tire drawbar pull during the traveling process

Fig. 16 shows the tire sinkage value as a function of the traveling distance under the 30% slip ratio condition. It can be seen that the tire sinkage value increases

dramatically at the initial stage due to the unbalance vertical force acting on the tire. Then its value fluctuates around the value of 45 mm and there are no abrupt fluctuations at the alternate point.

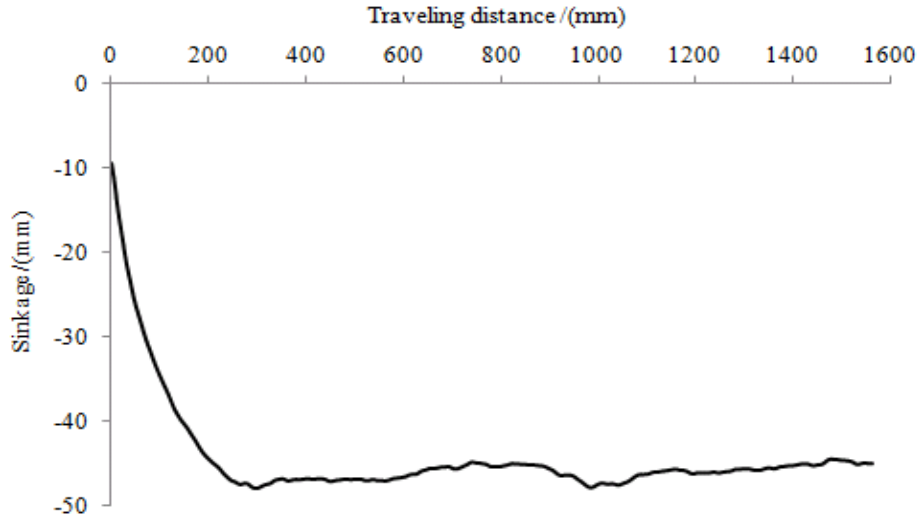
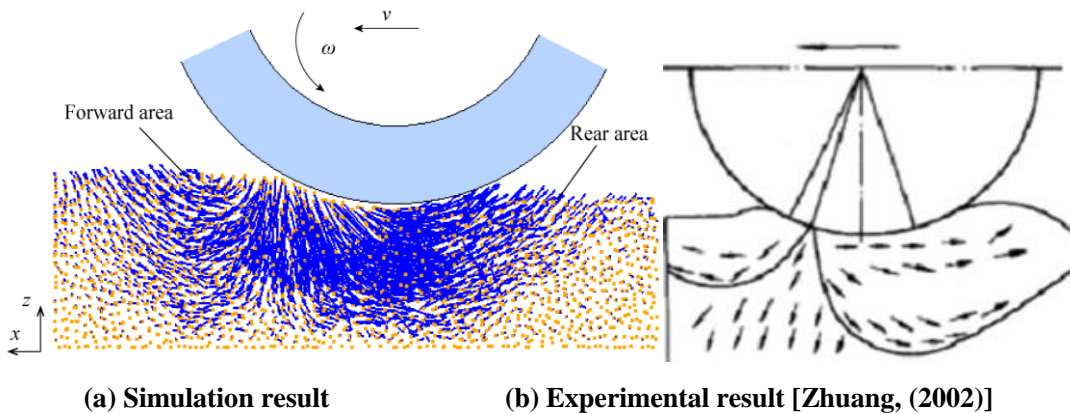


Figure 16. The tire sinkage during the traveling process

Fig. 17(a) presents the flow trend of the discrete elements in the X-Z plane under the rolling tire with 30% slip ratio. Herein, the velocity vectors of the elements are used to display their flow trend. It can be seen that the flow trend can be divided into two areas: the forward area flow in clockwise direction due to the bulldozing force of the tire and the rear area in anticlockwise direction because of the traction force of the rolling tire (digging effect). This result agrees qualitatively with the experimental result [Zhuang, (2002)] as illustrated in Fig. 17(b).



(a) Simulation result (b) Experimental result [Zhuang, (2002)]
Figure 17. Flow trend of the sand particles under a rolling tire

A constant angular velocity of 0.5 rad/s and corresponding translational velocity for different slip ratios according to Eq.(5) are loaded to the mass center of the tire to further analyze the influence of the slip ratio on the tire running behavior. Fig. 18 illustrates the tire equivalent sinkage values (the average sinkage value under each slip ratio) as a function of the slip ratios. It can be seen that the equivalent tire sinkage values are rise with the increase of the slip ratio. And the trend becomes steeper when the slip ratio is larger. This agrees qualitatively with the experimental results in [Shinone et al., (2010)]. However, the simulation results are larger than the experiment results. The possible reason is that the parameters in this study are decided by a trial and error preliminary computation to ensure the numerical stability at this stage. And the selection of the microscopic parameters among the discrete

elements has strong effects on its macroscopic mechanics.

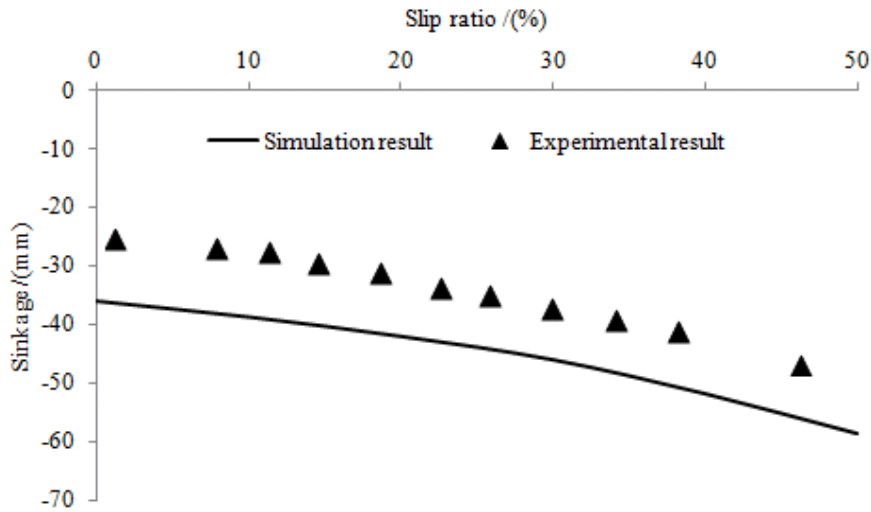


Figure 18. The relation between tire sinkage and slip ratio

Fig. 19 illustrates the equivalent values (the average drawbar pull value under each slip ratio) of the drawbar pull as a function of the slip ratios. It can be seen that the drawbar pull shows an increasing trend when the slip ratio is less than 25%, and its value tend to be stable when the slip ratio is larger than 25%. Such whole developing trend agrees qualitatively with the experimental result in [Shinone et al., (2010)]. It should be noticed that there is a large difference between the simulation results and the experimental results when the slip ratio is less than 15%. The possible reason for this phenomenon is the larger translational speed of the tire for the smaller slip ratio condition according to Eq. (8), and this leads to larger tire bulldozing resistance. The drawbar pull values have a little decrease after the slip ratio value is larger than 35%. This is because the bulldozing force is even larger due to the larger tire sinkage values under these slip ratio conditions. It should also be noticed that all the drawbar pull values are smaller than the experimental results because of the larger sinkage values, as shown in Fig. 19, which leads to larger bulldozing resistance.

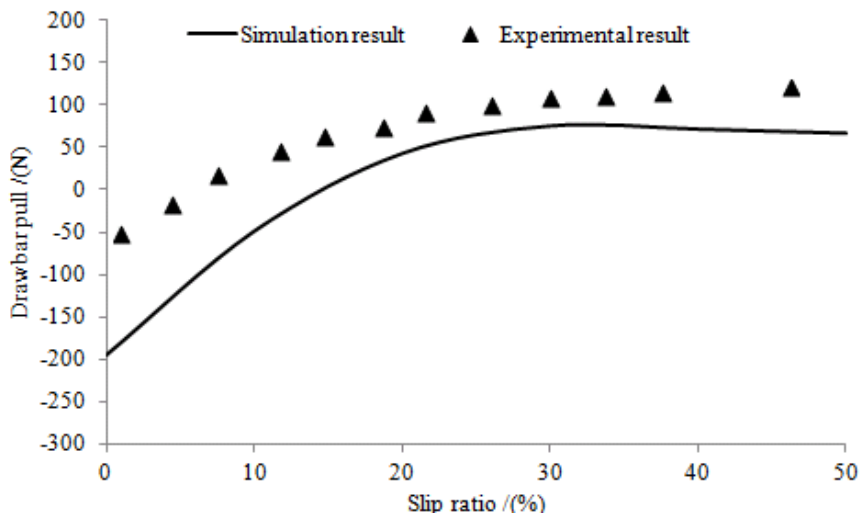


Figure 19. The relation between tire drawbar pull and slip ratio

4.5 Discussions

As can be seen from the Fig. 14, Fig. 15 and Fig. 16, the alternate moving road process is stable and effective for the simulation of tire running behavior on arbitrary

length sand roads.

As can be seen from Fig. 17, Fig. 18 and Fig. 19, the tire slip ratio has strong effect on its running behavior. The sinkage value of the tire rises with the increases of the slip ratio due to the tire traction effect (digging effect). This leads to the increase of the bulldozing resistance which is the main resistance for tire running on sand road. The drawbar pull shows a steeper increasing trend when the slip ratio is less than 25% and the values tend to be stable when the slip ratio is larger due to the dramatically increase of the resistance under these slip ratio conditions.

The comparisons between the simulation results and current experimental results show that the FEM/DEM is a straightforward and effective tool to investigate the tire running behavior on sand road, where the flow trend of the sand particles under a rolling tire, the drawbar pull and the sinkage of the tire and the dynamic parameters such as vertical acceleration value of the tire can be obtained expediently and reasonably.

5. Conclusions

From the above investigation, following results can be obtained:

(1) The Alternately Moving Road Method is proposed and applied to the FEM/DEM simulation of tire running behavior on the sand road. This method possesses the ability of simulating arbitrary length of sand road with constant discrete element numbers. Numerical simulation results show that the method is stable and effective.

(2) The tire running behavior such as the normal reaction force, tire drawbar pull, tire sinkage and flow trend of the sand particles can be obtained conveniently by the FEM/DEM. The comparisons between the simulation and current experimental results show that FEM/DEM is an effective and promising approach to simulate the tire running behavior on the sand terrain. The current research work is not only appropriate for the tire-sand interactions, but also suitable for the investigation of other terramechanics problems such as soil cultivation process.

Plans for the future work are to improve the accuracy of the method. The size effect of the discrete elements and the new discrete element interaction models considering the rolling resistance [Ai et al., (2011); Jiang et al., (2005); Kuhn and Bagi, (2004)] should be investigated.

Acknowledgements

This work was supported by The National Natural Science Foundation of China (NO. 11172104) and The International Cooperation Project of the Ministry of Science and Technology of China (NO. 2013DFG60080).

References

- Ai, J., Chen, J.-F., Rotter, J.M., Ooi, J.Y. (2011) Assessment of rolling resistance models in discrete element simulations, *Powder Technology* **206**, 269-282.
- Balevičius, R., Džiugys, A., Kačianauskas, R. (2004) Discrete element method and its application to the analysis of penetration into granular media, *Journal of Civil Engineering and Management* **1**, 3-14.
- BIRIS, S., Ungureanu, N., Maican, E., Murad, E., Vladut, V. (2011) FEM model to study the influence of tire pressure on agricultural tractor wheel deformations, *Engineering for rural development*, 27-27.
- Cuong, D.M., Zhu, S., Ngoc, N.T. (2013) Study on the variation characteristics of vertical equivalent

- damping ratio of tire–soil system using semi-empirical model, *Journal of Terramechanics*.
- David, A.H., John, F.P., Alex, C. (2001) Large scale discrete element modeling of vehicle-soil interaction, *International Journal for Numerical Methods in Engineering* **127**, 1027-1032.
- González Cueto, O., Iglesias Coronel, C.E., Recarey Morfa, C.A., Urriolagoitia Sosa, G., Hernández Gómez, L.H., Urriolagoitia Calderón, G., Herrera Suárez, M. (2013) Three dimensional finite element model of soil compaction caused by agricultural tire traffic, *Computers and Electronics in Agriculture* **99**, 146-152.
- Han, K., Peric, D., Crook, A.J.L., Owen, D.R.J. (2000) A combined finite/discrete element simulation of shot peening processes—Part I: studies on 2D interaction laws, *Eng Computation* **17**, 593-620.
- Jiang, M.J., Yu, H.S., Harris, D. (2005) A novel discrete model for granular material incorporating rolling resistance, *Computers and Geotechnics* **32**, 340-357.
- Khot, L.R., Salokhe, V.M., Jayasuriya, H.P.W., Nakashima, H. (2007) Experiment validation of distinct element simulation for dynamic wheel-soil interaction, *Journal of Terramechanics* **44**, 9.
- Knuth, M.A., Johnson, J.B., Hopkins, M.A., Sullivan, R.J., Moore, J.M. (2012) Discrete element modeling of a Mars Exploration Rover wheel in granular material, *Journal of Terramechanics* **49**, 10.
- Kuhn, M.R., Bagi, K. (2004) Contact rolling and deformation in granular media, *International journal of solids and structures* **41**, 5793-5820.
- Li, H., Schindler, C. (2013) Investigation of Tire-Soil Interaction with Analytical and Finite Element Method *Mechanics Based Design of Structures and Machines* **41**, 293-315.
- Moslem, N., Hossein, G. (2014) Numerical simulation of tire/soil interaction using a verified 3D finite element model, *Journal of Central South University* **21**, 817-821.
- Nakashima, H., Fujii, H., Oida, A., Momozu, M., Kawase, Y., Kanamori, H., Aoki, S., Yokoyama, T. (2007) Parametric analysis of lugged wheel performance for a lunar microrover by means of DEM, *Journal of Terramechanics* **44**, 153-162.
- Nakashima, H., Oida, A. (2004) Algorithm and implementation of soil-tire contact analysis code based on dynamic FE-DE method, *Journal of Terramechanics* **41**, 127-137.
- Nakashima, H., Takatsu, Y., Shinone, H. (2008) Analysis of tire tractive performance on deformable terrain by finite element-discrete element method, *Journal of computational science and technology* **4**, 423-434.
- Nakashima, H., Takatsu, Y., Shinone, H. (2009) FE-DEM analysis of the effect of tread pattern on the tractive performance of tires operating on sand, *Journal of Mechanical Systems For Transportation and Logistics* **2**, 55-65.
- Shinone, H., Nakashima, H., Takatsu, Y. (2010) Experimental analysis of tread pattern effects on tire tractive performance on sand using an indoor traction measurement system with forced-slip mechanism, *Engineering in Agriculture, Environment and Food* **3**, 61-66.
- Smith, W., Peng, H. (2013) Modeling of wheel-soil interaction over rough terrain using the discrete element method, *Journal of Terramechanics* **50**, 277-287.
- Williams, J.R., Perkins, E., Cook, B. (2004) A contact algorithm for partitioning N arbitrary sized objects, *Engineering Computations* **21**, 235-248.
- Zang, M.Y., Gao, W., Lei, Z. (2011) A contact algorithm for 3D discrete and finite element contact problems based on penalty function method, *Computational Mechanics* **48**, 541-550.
- Zhang, R., Liu, F., Zeng, G.Y., Li, J.Q. (2012) Research on dynamic simulation system of interactions between irregular rigid wheel and lunar soil simulant, CMGM-2012, China:Zhangjiajie, pp. 438-444.
- Zhao, C.L., Zang, M.Y. (2014a) Analysis of rigid tire traction performance on a sandy soil by 3D finite element-discrete element method, *Journal of Terramechanics*, (Submitted).
- Zhao, C.L., Zang, M.Y. (2014b) An improved discrete and finite element contact algorithm for the analysis of wheel-sand interaction, *Computers and Structures*, (submitted).
- Zhuang, J.D. (2002) Computational vehicle terramechanics, 1st ed. *CMP*, China.